Journal of Sound and Vibration 331 (2012) 5424–5434

Contents lists available at SciVerse ScienceDirect

Journal of Sound and Vibration

journal homepage: www.elsevier.com/locate/jsvi

Levenberg–Marquardt iterative regularization for the pulse-type impact-force reconstruction

Fergyanto E. Gunawan

Department of Industrial Engineering, Faculty of Engineering, Bina Nusantara (Binus) University, Jl. KH Syahdan 9, Kemanggisan, Jakarta 11480, Indonesia

ARTICLE INFO

Article history:
Received 18 November 2010
Received in revised form
4 June 2012
Accepted 14 July 2012
Handling Editor: L.G. Tham
Available online 16 August 2012

ABSTRACT

In this paper, we study the Levenberg–Marquardt algorithm with the trust region strategy to iteratively solve the ill-posed impact-force reconstruction problem. This particular problem is interesting because the impact-force particularly those of the pulse-type are difficult to be measured directly. In the present approach, the necessity of regularization is enforced by means of the trust region approach. This study mainly contributes a systematic approach to locate the optimal solution by tracking the Levenberg–Marquardt parameter. The proposed method is evaluated by solving two typical problem existed in the inverse problem of the impact-force reconstruction. Reasonable accurate impact-forces were produced from the both evaluations.

1. Introduction

The inverse analysis of an impact-force has presented researchers with a dilemma. The analysis is extremely useful because it allows us to inversely estimate the pulse-type impact-force, which is difficult to be measured directly. Unfortunately, the problem of inversely determining the pulse-type impact-force is ill-posed in sense of Hadamard's criteria [1]. The method of solution of the problem is difficult, its computational cost is high, and most important of all, it is difficult to obtain an accurate solution. The difficulty arises from the ill-posed nature of the governing equation; thus, some sort of numerical stabilization or regularization is necessary to produce a computable and acceptable solution [2]. The computational cost is relatively high by one or more orders because many solutions for various degrees of regularization have to be calculated, from which an optimal solution can be selected according to a specific objective function. Commonly, the objective function is a combination of a residual term and an error term. An accurate solution is also hard to find because the governing equation of the ill-posed problem tends to increase errors contained in data by several-folds depending on the severity of the problem. In a linear inverse problem, for an example, the perturbation analysis has shown that the error in the data propagates into the solution proportional with the magnitude of the condition number of the problem [3]; therefore, for the present problems that have condition number in order of 10^5, an extremely small error in the data can easily produce an erroneous solution without proper regulation.

The ill-conditioning nature arising in the inverse problems of the impact-force reconstruction has been recognized since early of 1980s [4,5]. Some earlier solutions [6–11] were developed on the basis of the Wiener filter [12], which basically minimizes the error in the solution without any attempt to regularize the solution. The standard solution method of the ill-posed problem, i.e., the singular value decomposition (SVD) method, has also been adopted for solving the ill-posed force reconstruction problem [13,14]. The SVD-based method is widely regarded as the best method, with respect to

E-mail addresses: f.e.gunawan@gmail.com, fgunawan@binus.edu

0022-460X/$ - see front matter © 2012 Elsevier Ltd. All rights reserved.
http://dx.doi.org/10.1016/j.jsv.2012.07.025

accuracy of the solution, to solve any ill-posed problem [2] because using the method, we can decompose the problem and the data into their spectral contents; hence, the effect of the data error to the solution can be minimized. However, the decomposition requires a relatively high computational cost, the highest among the direct solution methods [15]; thus, the SVD-based method is only feasible to be used to solve small-size inverse problems.

The Wiener filter is basically feasible and efficient to solve large-size inverse problems due to the existence of the fast Fourier transformation [16], but without a regularization, the solution provided by the method is often unacceptable unless the condition number is relatively small in order of few hundreds. For the reason, we proposed a regularized Wiener filter in Ref. [17] where an additional filter term was introduced to regularize the solution, and the filter parameters were optimally selected to minimize Tikhonov's objective function for the ill-posed problem. In addition, Tikhonov regularization has also been employed to estimate the impulse-type impact-force acting on a nonlinear system [18].

Rather different solution methods can be seen in Juang and Hu [19] and Leclere and Pezerat [20]. The former regularized the solution by controlling the vibration modes, and the latter adopted a low-pass filter approach where the equation of motion was resolved using the finite difference approach.

Furthermore, we proposed a number of solution methods [21–23], which in general, taking into account the possible profile of the impact-force as priori information of the solution. We approximated the impact-force profile, firstly, with a B-spline [21], then with a quadratic spline [22]—a lower order spline, and finally, with a new set of the basis functions that allows us to approximate accurately the loading and unloading phases of the impact-force profile [23].

The SVD-based method is only suitable for small-size inverse problems, and an iterative regularization is more desirable for the medium and large-size problems [2]. However, there are very limited developments in the iterative regularization particularly for reconstructing the pulse-type impact-force. In Ref. [24], we adopted the iterative regularization of the conjugate gradient (CG) method, and proposed a termination scheme that is suitable for the problems. The selection of the conjugate gradient method among many iterative methods was strengthened by Kurpisz and Nowak [25] whom assert that the iterative method of the conjugate-gradient type is the most suitable for inverse analysis. Two main reasons are: the CG method, unlike the Newton-based methods, does not require the inverse of the Hessian matrix or its approximation, which for the ill-posed problem is difficult to compute accurately, and the second reason is: the CG method has inherent regularization where the degree of regularization decreases by increasing the iteration.

Although the CG method has some advantages over the Newton-based methods, the latter converge faster than the former as shown in many studies particularly in solving well-posed problems. In this paper, we extend the Levenberg–Marquardt (LM) method, a variant of the Gauss–Newton methods, to solve the ill-posed pulse-type impact-force inverse problem in conjunction with a trust region strategy. The trust region strategy is used to stabilize the iteration in the LM method. Furthermore, we also study the effects of the trust region parameters to the convergence of the LM method. Finally, we evaluate the solution method by solving two typical problems in the impact-force reconstruction.

2. Governing equation of the impact-force reconstruction

From the mathematical standpoint, the force reconstruction problem discussed in this paper involves a convolution integral equation of

$$\int_0^t h(t-\tau)f(\tau)\,\mathrm{d}\tau = e(t), \tag{1}$$

where $h(t)$ is the impulse response function, $f(t)$ is the impact-force, and $e(t)$ is the induced elastic response. The integral equation can easily be expressed in the form of the finite dimensional linear system as follows:

$$\mathbf{Hf} = \mathbf{e}, \tag{2}$$

which can directly be obtained from the integral equation via a numerical discretization. The discretization is simply by, firstly, representing the continuous independent variable t with $t_i = (i-1)\Delta t$ where i is an integer index in $[0,(N-1)]$ and Δt is a sampling time. Secondly, the function $f(t)$, $e(t)$, and $h(t)$ must be re-sampled at those discrete time. The discretization of the function $h(t)$ will naturally lead to a matrix, so-called the convolution matrix $\mathbf{H}$, that has Toeplitz structure [26–28].

It is well-known that for the ill-posed problem, the solution $\mathbf{f}$ of the linear system of Eq. (2) is very sensitive to data errors. An attempt to solve directly the equation will likely lead to an erroneous solution. Obtaining a meaningful solution is possible by using some sort of numerical regularization or stabilization, among which Tikhonov regularization [2]:

$$\min_{\mathbf{f}}[\|\mathbf{Hf}-\mathbf{e}\|_2^2+\lambda^2\|\mathbf{f}\|_2^2], \tag{3}$$

where λ is the regularization parameter, has outstanding popularity.

3. Levenberg–Marquardt method

The Levenberg–Marquardt algorithm [29,30] is designed to address the problem of the nonlinear least squares. This paper discusses a special case, that is a linear least squares problem with the Toeplitz structure of the Jacobian matrix. In this section, we adopt a notation system that widely used in the theory of optimization, although few notations conflict to

those that usually used in publications of the force reconstruction; but the meaning of each notation should be clear by referring to its context.

The problem is to find a solution of $\mathbf{Ax}=\mathbf{b}$ that minimizing the least squares function, $f(\mathbf{x})$:

$$f(\mathbf{x})=\tfrac{1}{2}\mathbf{r}(\mathbf{x})^T\mathbf{r}(\mathbf{x}), \tag{4}$$

where $\mathbf{r}(\mathbf{x})$ is the residue such that $\mathbf{r}(\mathbf{x})=\mathbf{Ax}-\mathbf{b}$. It is easy to show that the gradient of Eq. (4) is

$$\mathbf{g}(\mathbf{x})=\nabla f(\mathbf{x})=\mathbf{A}^T\mathbf{r}(\mathbf{x}). \tag{5}$$

A rapid reduction of $f(\mathbf{x})$ can be obtained by updating $\mathbf{x}$ in the Gauss–Newton direction:

$$\mathbf{s}(\mathbf{x})=-(\mathbf{A}^T\mathbf{A})^{-1}\ \mathbf{g}(\mathbf{x}) \tag{6}$$

Eq. (6) can be solved if $\mathbf{A}^T\mathbf{A}$ is not only a matrix that has full column rank but also must be uniformly bounded and well conditioned.

For the ill-posed problems, the Levenberg–Marquardt method stabilizes Eq. (6) by adding a regularization parameter or a Levenberg–Marquardt parameter, v, such that

$$\mathbf{s}(\mathbf{x})=-(\mathbf{A}^T\mathbf{A}+v\mathbf{I})^{-1}\ \mathbf{g}(\mathbf{x}), \tag{7}$$

where $\mathbf{I}$ is the identity matrix. With respect to the general optimization approach, the regularization is applied during the line search strategy. Selection of the regularization parameter v is the subject of the next discussion. We note that, in this paper, Eq. (7) is solved using the QR decomposition.

3.1. Regularization parameter by the trust region method

Let that $\mathbf{x}_c$ is the current point or solution. The quadratic model of the linear least squares objective function allows us to predict the next solution, $\mathbf{x}_+$, based on Newton's approach. The approach theoretically estimates the reduction of the objective function, Δf_{theo}, by

$$\Delta f_{\text{theo}}=-\mathbf{g}(\mathbf{x}_c)^T(\mathbf{x}_c-\mathbf{x}_+), \tag{8}$$

while the actual reduction, Δf_{act}, can be easily obtained by

$$\Delta f_{\text{act}}=f(\mathbf{x}_c)-f(\mathbf{x}_+). \tag{9}$$

The regularization parameter, v, should be adjusted such that $\mathbf{x}_+$ reduces $f(\mathbf{x})$ sufficiently. The sufficiency is measured by a variable, r, which is a relative magnitude of the actual reduction over the theoretical reduction:

$$r=\frac{\Delta f_{\text{act}}}{\Delta f_{\text{theo}}}. \tag{10}$$

For the ill-posed problem, the small v tends to produce large $\mathbf{x}_+$ in sense of its Euclidian norm, which in turn increases Δf_{theo}, and consequently, reduces the r. The regularization parameter v is adjusted by use of a trust region approach that adjusts v by comparing the r to the trust region parameters: μ_0, μ_{low}, and μ_{high}.

If r is smaller than μ_0, the solution contains the noise excessively, then v will be increased by a factor of ω_{up}, and $\mathbf{x}_+$ is recomputed by the following steps:

$$\mathbf{A}_c=\mathbf{A}^T\mathbf{A}+v\mathbf{I},$$

and

$$\mathbf{d}=\mathbf{A}_c^{-1}\ \mathbf{g}(\mathbf{x}_c),$$

and finally,

$$\mathbf{x}_+=\mathbf{x}_c-\mathbf{d}. \tag{11}$$

The LM parameter is also increased by the same factor if r lies between μ_0 and μ_{low}; but for such a case, $\mathbf{x}_+$ is accepted as the next solution, $\mathbf{x}^{k+1}$. The LM parameter is optimal if it gives r in the interval of μ_{low} and μ_{high}; and it is reduced if r is larger than μ_{high}. Fig. 1 graphically describes the regulation.

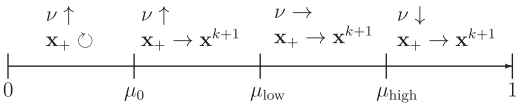

Fig. 1. Trust region method for selection of the LM parameter, v. The symbol $v\downarrow$ means the parameter is reduced by a factor of ω_{down}; $v\uparrow$ denotes the parameter is increased by a factor of ω_{up}; $v\rightarrow$ means the parameter is kept; and $\mathbf{x}\circlearrowleft$ denotes that the point is recomputed. The factors ω_{down} and ω_{up} are the penalty parameters.

3.2. Termination criterion

The most difficult problem in solving the ill-posed problems is finding an appropriate regularization parameter. According to Kilmer and O'Leary [31], the existing method such as the discrepancy principle, the generalized cross validation (GCV) method, and the L-curve method have severe flaws. Finding an appropriate regularization parameter becomes a subject of interest of many publications especially in connection with the iterative solution method.

In Ref. [24], we proposed a variant of the discrepancy principle that used to terminate the conjugate gradient iteration. It shows that the CG method exhibits a semi-convergent behavior that the iteration seemingly convergences in the beginning of the iteration before they eventually turn to diverge. Such a phenomenon happens because the method reduces the degree of regularization continuously along iteration. As far as the solution, $\mathbf{x}^k$, is not too close to the true solution, the residual norm, $\|\mathbf{A}\mathbf{x}^k-\mathbf{b}\|$, is quite large and the solution norm, $\|\mathbf{x}^k\|$, is relatively small, negligible as compared to the size of the residual. By increasing the iteration, $\|\mathbf{A}\mathbf{x}^k-\mathbf{b}\|$ shrinks, while $\|\mathbf{x}^k\|$ increases. Eventually, the iteration will provide an optimal solution. A regularization parameter that slightly lower than its optimal value will increase $\|\mathbf{x}^k\|$ abruptly, and then further iteration will increase $\|\mathbf{x}^k\|$ significantly. Therefore, the optimal iteration can be easily detected by $\|\mathbf{A}\mathbf{x}^k-\mathbf{b}\|_2^2+\|\mathbf{x}^k\|_2^2 \le \|\mathbf{A}\mathbf{x}^{k+1}-\mathbf{b}\|_2^2+\|\mathbf{x}^{k+1}\|_2^2$.

A smooth evolution of the regularization parameter also appeared in an iterative solution method by use of a modified Newton method as proposed in Ref. [32]. In addition to its smoothness, the sequence of the regularization parameter approaches the optimal regularization from one side. Hence, the iteration can be terminated when the regularization parameter is steady.

None of such smoothness can be expected from the present approach because the trust region method suddenly changes the regularization parameter by an amount of the penalty parameters: ω_{down} and ω_{up}. However, at the steady state, we can expect that the regularization parameter fluctuates harmonically in a certain range. In Section 4.1, we empirically devise a method to find the optimal regularization parameter.

For the Levenberg–Marquardt method, Hanke [33] presented a theoretical development that shows that the discrepancy principle given in Eq. (12) provides a well-defined and stable approximation of $\mathbf{A}\mathbf{x}=\mathbf{b}$, with $\tau>1$ is another parameter and δ is a parameter that describes the noise:

$$\|\mathbf{A}\mathbf{x}^k-\mathbf{b}\| \le \tau\delta. \tag{12}$$

For the practical application, it is difficult to use such an approach because lack of information of δ, and accuracy of the solution strongly depends on selection of τ.

4. Numerical studies

4.1. Single degree of freedom system

4.1.1. Model description

Consider a single degree of freedom system (SDOF) that is subjected to an impact-force $f(t)$. The system consists of a mass, a spring and a damper. The impulse response function of the system can be expressed as $h(t)=1/(m\omega_d)e^{\zeta\omega_n t}\sin(\omega_d t)$, where ω_n and ω_d denote the circular natural and the circular damped frequencies. Both the parameters can be computed by $\omega_n=\sqrt{k/m}=2\pi f_n$ and $\omega_d=\omega_n\sqrt{1-\zeta^2}$. In the present study, the following data are selected: $m=1.0$ kg, $k=1\times10^{11}$ N/m, and $\zeta=0.2$.

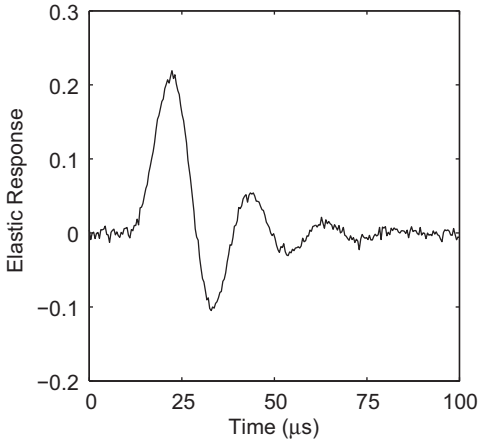

Fig. 2. The normalized elastic response of the SDOF system corrupted by the Gaussian random noise of variance of 2 percent.

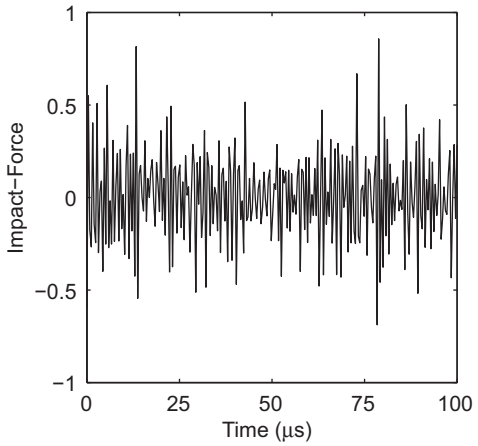

Fig. 3. The least squares solution of the SDOF system without regularization.

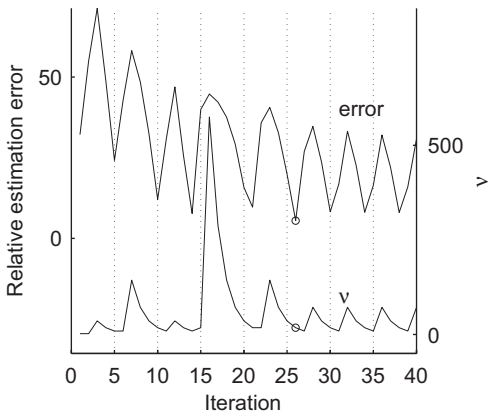

Fig. 4. Evolution of the Levenberg–Marquardt parameter, ν, and the relative estimation error along iteration.

Fig. 2 shows the elastic response data that is corrupted by the Gaussian random noise of variance of 2 percent of the maximum of the elastic strain data. The data plotted in the figure were normalized by its Euclidian norm. The data were sampled at a time-step of 0.4 μs. The impact-force is a shifted full-sine function. To provide a sense of the ill-posedness of the problem, Fig. 3 shows the dimensionless estimated impact-force that is directly obtained by solving Eq. (2) by means of the least squares method without a regularization.

4.1.2. Convergence of the Levenberg–Marquardt method

We study various parameters that are crucial for determining the termination criterion in the Levenberg–Marquardt iteration. Those parameters are the objective function, the natural criterion, the ratio r, and the regularization parameter, ν. However, during the analysis we kept in mind that the regularization parameter ν should be minimum to maintain the originality of the problem. In this study, we adopt Ref. [34] for the trust region parameters as follows: $\mu_0 = 0.1$, $\mu_{\text{low}} = 0.25$, $\mu_{\text{high}} = 0.75$, $\omega_{\text{up}} = 2$, and $\omega_{\text{down}} = 0.5$; and perform the analysis for 200 iterations.

The computational results show that the objective function and the gradient norm steadily decrease by increasing the iteration, while the relative estimation error that was defined by

$$\text{Relative error} = \frac{\|\mathbf{x}_{\text{exact}} - \mathbf{x}_{\text{estimation}}\|}{\|\mathbf{x}_{\text{exact}}\|}$$

decreases and then harmonically oscillates (see Fig. 4). Thus, the objective function and the gradient norm can hardly be used as the termination criterion.

In addition to the estimation error, Fig. 4 also shows the history of the regularization parameter, ν. When the number of iterations is larger than 25, the regularization parameter is also oscillating harmonically. The harmonic oscillation phenomenon of the regularization parameter can be easily understood by observing the ratio r that is presented in Fig. 5.

Those figures show that at the steady condition, the penalty parameter ω_{up} regularly penalized the regularization parameter when the regularization parameter becomes too small such that the ratio r is smaller than μ_0. As the iteration

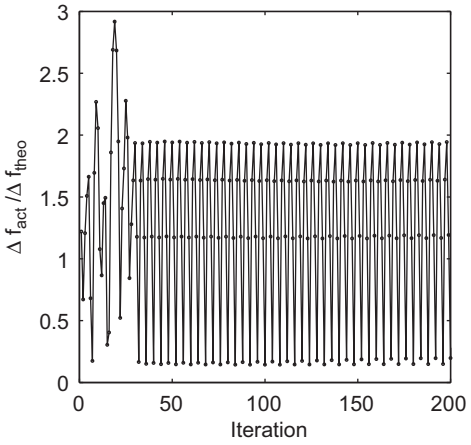

Fig. 5. Evolution of the ratio, r, along Levenberg–Marquardt along iteration.

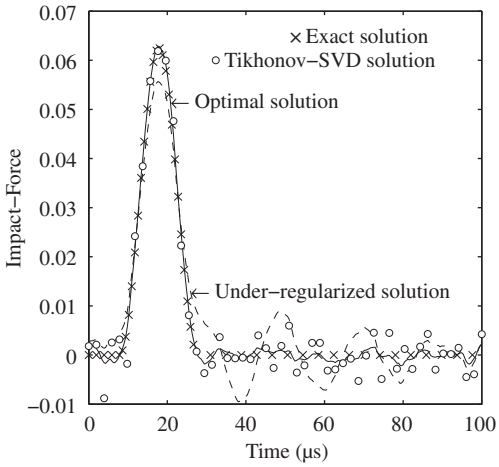

Fig. 6. The exact solution, the Tikhonov-SVD solution, the optimal estimated solution and the under-regularized solution.

continues, the trust region method reduces the regularization parameter gradually until μ_0 is violated, then the previous process is repeated. Therefore, it is natural to select the best solution that has the smallest regularization parameter but do not violate the minimum trust region parameter. This criterion provides a regularization parameter that is marked as a circle, '○', in Fig. 4. In the same figure, we can see that this regularization parameter provides a solution that has the smallest relative estimation error, and Fig. 6 shows the associated estimated impact-force. The figure also shows the under-regularized solution that was obtained by reducing the regularization parameter slightly, and the solution obtained by the Tikhonov-SVD method.

The nature of the convergence depicted in Fig. 4 is rather similar to that is shown in Fig. 5 of Ref. [35] where an adaptive Tikhonov regularization method is developed and employed to solve a nonlinear finite element model updating problem.

4.1.3. *Effect of the trust region parameters*

We also study various configurations of the trust region parameters: μ_0, μ_{low}, μ_{high}, ω_{up}, and ω_{down}. Fig. 7 shows a notable result that the oscillation of the estimation error is damped down rapidly when μ_0 is increased from 0.1 to 0.25.

4.2. *Pre-cracked one-point bend specimen*

4.2.1. *Model description*

Consider a one-point bend specimen that was depicted in Fig. 8. By using the Euler–Bernoulli beam theory, Kishimoto et al. [36] have derived a convolution integral equation that relates the stress intensity factor $K_I(t)$ to the impact-force $f(t)$; and in the other side, Dally and Sanford [37] show that the stress intensity factor is proportional to the strain at near the crack-tip; therefore, the impact-force can be related to the strain at near the crack-tip by the convolution integral equation.

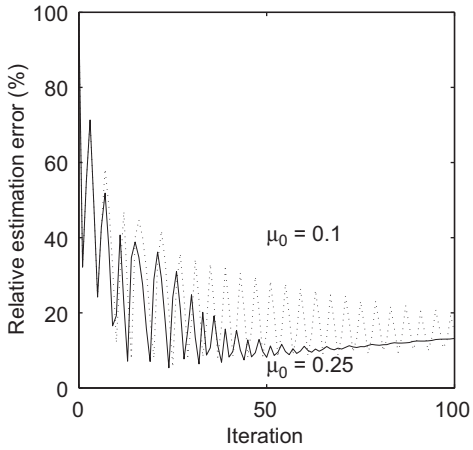

Fig. 7. Effect of a trust-region parameter of μ_0 to the estimation error.

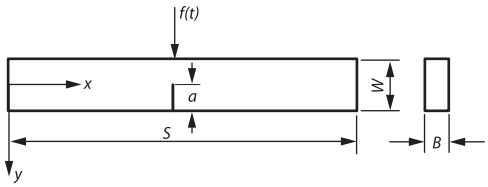

Fig. 8. One-point bend specimen.

According to Kishimoto et al. [36], the impulse response function of the Euler–Bernoulli beam can be expressed as

$$h(\xi,t)=\frac{t}{\rho AS}+\sum_{m=1}^{\infty}\frac{Y_m(\frac{1}{2})Y_m(\xi)}{\omega_m W_m S}\sin(\omega_m t), \tag{13}$$

where $\xi=x/S$, ρ is the density, S is the specimen span, a is the crack length, A is the cross-sectional area, $Y_m(\xi)$ are the normal modes, and ω_m are the natural angular frequencies. The normal modes $Y_m(\xi)$ are expressed as

$$Y_0(\xi)=\text{const},$$

$$Y_m(\xi)=\left(\cos\frac{\lambda_m}{2}-\cosh\frac{\lambda_m}{2}\right)(\cos\lambda_m\xi+\cosh\lambda_m\xi)+\left(\sin\frac{\lambda_m}{2}+\sinh\frac{\lambda_m}{2}\right)(\sin\lambda_m\xi+\sinh\lambda_m\xi).$$

And the natural frequencies are

$$\omega_0^2=0,$$

$$\omega_m^2=\left(\frac{\lambda_m}{S}\right)^2\frac{EI}{\rho A},$$

where E is the elastic modulus, I is the area of moment of inertia of the gross cross-section, and λ_m is the m-th root of the following equation:

$$\cos\frac{\lambda_m}{2}\sinh\frac{\lambda_m}{2}+\sin\frac{\lambda_m}{2}\cosh\frac{\lambda_m}{2}+\frac{DI}{2S}\lambda_m\left(\cos\frac{\lambda_m}{2}\cosh\frac{\lambda_m}{2}-1\right)=0. \tag{14}$$

The D in Eq. (14) is defined as

$$D=\frac{2(1-\nu^2)W}{I}V(a/W),$$

where

$$V(\alpha)=\left(\frac{\alpha}{1-\alpha}\right)^2(5.58-19.57\alpha+36.82\alpha^2-34.94\alpha^3+12.77\alpha^4).$$

Having the impulse response function $h(\xi,t)$, then one can calculate the displacement on the neutral plane by

$$u(\xi,t)=\int_0^t f(\tau)h(\xi,t-\tau)\,\mathrm{d}\tau, \tag{15}$$

which, further, can be related to the stress intensity factor by

$$K_I(t) = k_d[u(\tfrac{1}{2},t) - u(0,t)], \tag{16}$$

where

$$k_d = \frac{K_s}{f(t)\sum_{m=1}^{\infty} \dfrac{Y_m^2(\frac{1}{2})}{\omega_m^2 W_m S}}, \quad W_m = 2\rho A \int_0^{1/2} Y_m^2(\xi)\, \mathrm{d}\xi,$$

and $\alpha = a/W$.

The K_s is the stress intensity factor for a three-point-bend specimen, and it is written as

$$K_s = \frac{f(t)S}{BW^{3/2}g(\alpha)},$$

with

$$g(\alpha) = \frac{3\alpha^{1/2}[1.99 - \alpha(1-\alpha)(2.15 - 3.93\alpha + 2.7\alpha^2)]}{2(1+2\alpha)(1-\alpha)^{3/2}}.$$

The dynamic stress intensity factor can also be measured experimentally by using the gage method of Dally and Sanford [37]:

$$K_I(t) = E\varepsilon_{x''}(t)\sqrt{\tfrac{8}{3}\pi r}, \tag{17}$$

where $\varepsilon_{x''}(t)$ is the strain-time history measured using a strain-gage that bonded ahead of the crack-tip (see Fig. 9). The r is a distance from the crack-tip to the gage position.

4.2.2. The finite element analysis

The impact event of the one-point bend specimen with an impactor was simulated numerically by means of the finite element method on ANSYS/LS-DYNA finite element package. In this event, the both impactor and specimen were made of steel material having an elastic modulus and density of 200 GPa and 8100 kg/m^3, respectively.

The both were discretized using solid element-type, `SOLID164`, with eight nodes per element, and each node is having three degree of freedoms (u_x, u_y, and u_z) [38]. Fig. 10 shows the detailed finite element mesh of the impactor and the specimen; Only a quarter of the specimen and the impactor were modeled due to symmetry.

The geometry of the one-point specimen is 10 mm wide, 10 mm high, and 100 mm long. The crack in the specimen is assumed to be 5 mm in length. The impactor is 10 mm high and 50 mm long. It has a round end, as shown in Fig. 10, with a radius of 5 mm.

Initially, the impactor touched the specimen along the impact line, and then, all nodes on the impactor were accelerated with the same initial velocities of 30 m/s. The symmetric constraints were applied to all nodes laying on the symmetric planes of the impactor and specimen.

In the simulation, a strain-gage is assumed to be bonded at 2 mm ahead of the crack-tip and at an orientation of 45° following suggestion of Rizal and Homma [39].

The element mesh-size and the analysis time-step were adjusted such that a realistic impact event was obtained. This could be assessed by evaluating the depth of the penetration of the impactor onto the specimen.

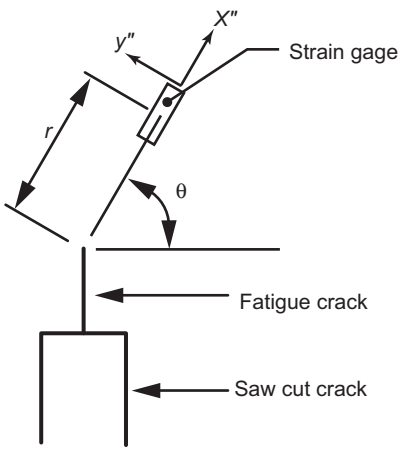

Fig. 9. The location of the strain-gage in the method of Dally and Sanford.

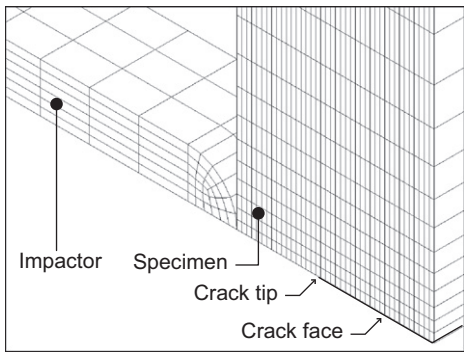

Fig. 10. Finite element mesh of an impact on a one-point bend specimen.

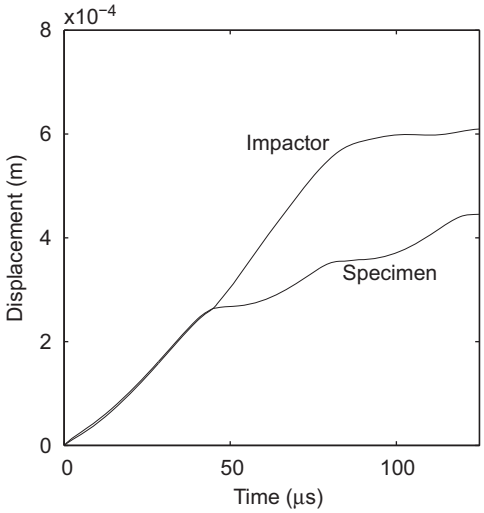

Fig. 11. Displacement of the impactor and the specimen at the impact-point.

Fig. 11, for an example, shows the displacements of the two coincided nodes, one on the impactor and the other on the specimen, during the impact event. The figure indicates that the impactor fully contacted the specimen for a duration of about 50 μs before the impactor and specimen lost contact. This duration is equivalent with the time for the longitudinal waves to propagate on the impactor from the impact end and return to the same end. Therefore, we concluded that the finite element analysis reasonably reproduced the impact event.

4.2.3. Inverse analysis results

In this section, we present the results of the inverse analysis that reconstructed the applied impact-force based on the elastic strain data recorded at the gage location obtained from the previous finite element analysis. The elastic strain data are reproduced in Fig. 12 after a normalization with the Euclidian norm of the data.

Based on those data, the Levenberg–Marquard algorithm, then, applied to compute the impact-force; the results are presented in Figs. 13 and 14. The regularization parameter, v, rapidly reached its harmonic state, which clearly indicates that the optimal solution is that at the 6-th iteration of the LM method.

Meanwhile, Fig. 14 shows the corresponding optimal solution by the Levenberg–Marquard method. On the same figure, the impact-force that is obtained from the finite element analysis is also presented. Evidently, the figure shows that the solution is acceptable within a relative estimation error of 9 percent at the peak of the force.

5. Conclusion

Recent study on the ill-posed impact-force reconstruction problems has provided a new technique, on the basis of the Levenberg–Marquardt iterative solution method, to find the optimal solution of the problem iteratively. Current finding suggests that the evolution of the regularization parameter, v, during iteration provides information of the iteration associated with the optimal solution. The method, unlike the SVD-based method, requires significantly less the computer

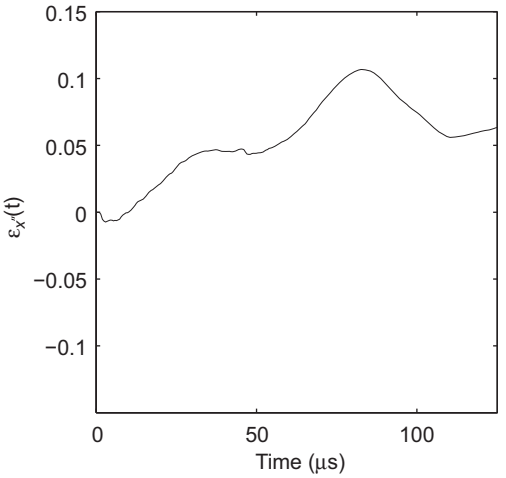

Fig. 12. The impulse response function and the elastic strain near the crack-tip of an impacted one-point bend specimen.

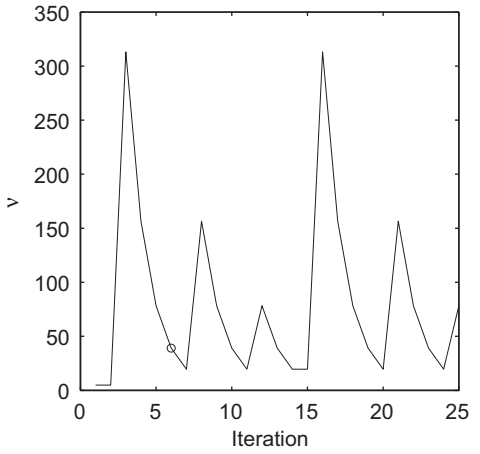

Fig. 13. Evolution of the Levenberg–Marquardt parameter, ν, along iteration for case of a one-point bend specimen.

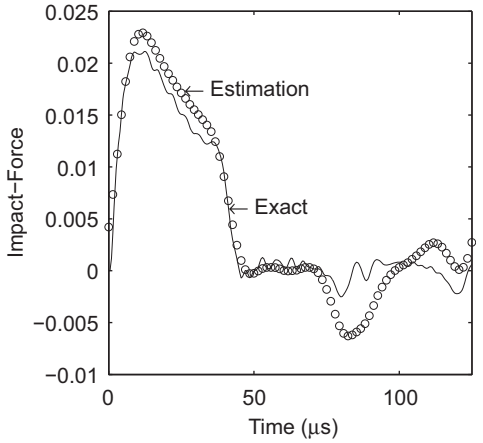

Fig. 14. The optimal estimated impact-force by the Levenberg–Marquardt method and the exact impact-force that is obtained from a finite element analysis. The data are normalized by their Euclidian norms.

memory; therefore, for a problem that cannot be solved by the SVD-based method due to limitation on the computer memory, the problem should be able to address using the proposed method. However, one should note that the current proposal, similar with the CG method (see for examples: [21,24]), requires us to maintain the history of the solution along

the iteration. It is still not clear which methodology, the CG method or the LM method, is more effective to solve the present ill-posed problem. The CG method has a quadratic convergence rate during the iteration before an optimal solution is reached; meanwhile, the LM method convergence rate varies along the iteration depending on the trust region parameter v.

References

[1] A.N. Tikhonov, V.A. Arsenin, *Solution of Ill-posed Problem*, Winston & Sons, 1977.
[2] P.C. Hansen, *Rank Deficient and Discrete Ill Posed Problems, SIAM Monograph on Mathematical Modeling and Computation*, SIAM, Philadelphia, 1998.
[3] J.W. Demmel, *Applied Numerical Linear Algebra*, SIAM, 1997.
[4] K.K. Stevens, Force identification problems—an overview, *SEM Spring Conference on Experimental Mechanics*, SEM, 1987, pp. 838–844.
[5] J.M. Starkey, G.L. Merrill, On the ill-conditioned nature of indirect force-measurement techniques, *Journal of Modal Analysis* 7 (1989) 103–108.
[6] H. Inoue, K. Kishimoto, T. Shibuya, T. Koizumi, Estimation of impact load by inverse analysis (optimal transfer function for inverse analysis), *JSME International Journal* 35 (4) (1992) 420–427.
[7] H. Inoue, H. Ishida, K. Kishimoto, T. Shibuya, Measurement of impact load by using an inverse analysis technique (comparison of methods for estimating the transfer function and its application to the instrumented Charpy impact test), *JSME International Journal—Series I* 34 (4) (1991) 453–458.
[8] H. Inoue, T. Shibuya, T. Koizumi, Measurement of Impact Load in Charpy Test by using Deconvolution Procedure, in: *Proceedings of the 9th International Conference of Experimental Mechanics*, Aug 1990, pp. 1989–1998.
[9] H. Inoue, K. Kishimoto, T. Shibuya, K. Harada, Regularization of numerical inversion of the Laplace transform for the inverse analysis of impact force, *JSME International Journal, Series A, Solid Mechanics and Material Engineering* 41 (4) (1998) 473–479.
[10] M.T. Martin, J.F. Doyle, Impact force identification from wave propagation responses, *International Journal of Impact Engineering* 18 (1) (1996) 65–77.
[11] J.F. Doyle, Force identification from dynamic responses of a bimaterial beam, *Experimental Mechanics* 33 (March (1)) (1993) 64–69.
[12] N. Wiener, *Extrapolation, Interpolation, and Smoothing of Stationary Time Series*, John Wiley & Sons, 1949.
[13] E. Jacquelin, A. Bennani, P. Hamelin, Force reconstruction: *analysis and regularization of a deconvolution problem*, *Journal of Sound and Vibration* 265 (2003) 81–107.
[14] Yi. Liu, W. Steve˜Shepard˜Jr., Dynamic force identification based on enhanced least squares and total least-squares schemes in the frequency domain, *Journal of sound and vibration* 282 (2005) 37–60.
[15] G.H. Golub, C.F.V. Loan, *Matrix Computation*, 2nd edition, The Johns Hopkins University Press, 1996.
[16] E.O. Brigham, *The Fast Fourier Transform*, Prentice-Hall, Inc., Englewood Cliffs, NJ, 1974.
[17] F.E. Gunawan, H. Homma, Y. Kanto, Time and frequency domain iterative regularization for inverse analysis of an instrumented one-point bend specimen, *Key Engineering Materials; Fracture and Strength of Solids VI* 306–308 (2005) 649–655. 〈http://www.scientific.net/KEM.306-308.649〉.
[18] T. Jang, H. Baek, S. Han, T. Kinoshita, Indirect measurement of the impulse load to nonlinear system from dynamic responses: *inverse problem formulation*, *Mechanical Systems and Signal Processing* 24 (2010) 1665–1681.
[19] X.Q. Jiang, H.Y. Hu, Reconstruction of distributed dynamic loads on a thin plate via mode-selection and consistent spatial expression, *Journal of Sound and Vibration* 323 (3–5) (2009) 626–644. URL 〈http://linkinghub.elsevier.com/retrieve/pii/S0022460X09000091〉.
[20] Q. Leclere, C. Pezerat, Vibration source identification using corrected finite difference schemes, *Journal of Sound and Vibration* 331 (6) (2012) 1366–1377. URL 〈http://www.sciencedirect.com/science/article/pii/S0022460X11008807〉.
[21] F.E. Gunawan, H. Homma, Y. Kanto, Two-step b-splines regularization method for solving an ill-posed problem of impact-force reconstruction, *Journal of Sound and Vibration (Scopus indexed)* 297 (2006) 200–214, http://dx.doi.org/10.1016/j.jsv.2006.03.036.
[22] F.E. Gunawan, H. Homma, Impact-force estimation by quadratic spline approximation, *Journal of Solid Mechanics and Materials Engineering* 2 (2008) 1092–1103, http://dx.doi.org/10.1299/jmmp.2.1092.
[23] F.E. Gunawan, H. Homma, A solution of the ill-posed impact-force inverse problems by the weighted least squares method, *Journal of Solid Mechanics and Materials Engineering (Scopus indexed)* 2 (2) (2008) 188–198, http://dx.doi.org/10.1299/jmmp.2.188.
[24] F.E. Gunawan, H. Homma, Efficient iterative solution for large inverse problem, *JSME International Journal Series A: Solid Mechanics and Material Engineering (Scopus indexed)* 47 (2) (2004) 130–137, http://dx.doi.org/10.1299/jsmea.47.130.
[25] K. Kurpisz, A.J. Nowak, *Inverse Thermal Problems*, Computational Mechanics Publications, 1995.
[26] G.M. Wing, *A Primer on Integral Equations of the First Kind*, SIAM, 1991.
[27] C.W. Groetsch, *The Theory of Tikhonov Regularization for Fredholm Equation of the First Kind*, Pitman, Boston, 1984.
[28] P. Hansen, Deconvolution and regularization with Toeplitz matrices, *Numerical Algorithms* 29 (2002) 323–378.
[29] K. Levenberg, A method for the solution of certain nonlinear problem in least squares, *Quarterly of Applied Mathematics* 4 (1944) 164–168.
[30] D.W. Marquardt, An algorithm for least-squares estimation of nonlinear parameters, *Journal of the Society for Industrial Applied Mathematics* 11 (1963) 431–441.
[31] M.E. Kilmer, D.P. O'Leary, Choosing regularization parameters in iterative methods for ill-posed problems, *SIAM Journal on Matrix Analysis and Applications* 22 (2001) 1204–1221.
[32] J. Kamm, J.G. Nagy, A total least squares method for Toeplitz systems of equations, *BIT* 38 (1997) 560–582.
[33] M. Hanke, A regularizing Levenberg–Marquardt scheme, with applications to inverse groundwater filtration problems, *Inverse Problems* 13 (1997) 79–95.
[34] C.T. Kelley, *Iterative Methods for Optimization*, Society for Industrial and Applied Mathematics, 1999.
[35] X.Y. Li, S.S. Law, Adaptive Tikhonov regularization for damage detection based on nonlinear model updating, *Mechanical Systems and Signal Processing* 24 (6) (2010) 1646–1664. URL 〈http://linkinghub.elsevier.com/retrieve/pii/S088832701000052X〉.
[36] K. Kishimoto, Y. Fujino, S. Aoki, M. Sakata, A simple formula for the dynamic stress intensity factor of an impacted freely-supported bend specimen, *JSME International Journal Series I* 33 (1990) 51–55.
[37] J.W. Dally, R.J. Sanford, Strain-gage methods for measuring the opening-mode stress intensity factor k_{IC}, *Experimental Mechanics* 27 (1987) 381–388.
[38] ANSYS LS-DYNA User's Guide, release 11 Edition.
[39] S. Rizal, H. Homma, Dimple fracture under short pulse loading, *International Journal of Impact Engineering* 24 (2000) 69–83.